Real Time Orbit Determination with Different Force Fields

VIVIAN MARTINS GOMES, ANTONIO F. B. A. PRADO, HÉLIO KOITI KUGA
National Institute for Space Research – INPE - DMC
Av. Dos Astronautas 1758 – São José dos Campos – SP – 12227-010
BRAZIL
vivian.gomes@uol.com.br; prado@dem.inpe.br; hkk@dem.inpe.br

Abstract: The Global Positioning System (GPS) is a satellite navigation system that allows the users to determine 3D positioning and the time with high precision. Its main purposes are: aid to radionavigation in three dimensions with high precision positioning, navigation in real time, time synchronization, global coverage and quick acquisition of data signal sent by the GPS satellites. In this work, it is proposed to estimate, in real time, an orbital state vector composed by position, velocity, bias and drift of the GPS receiver clock on board satellites by processing the raw navigation solution obtained by the on-board receiver. In this work the Kalman filter is used to estimate the state vector based on the stepwise incoming navigation solution from the receiver. The Kalman filter is used due to its robustness in real time applications, without unnecessary storage of observations, as they can be processed while being collected. The filter dynamic model includes perturbation due to geopotential, solar radiation pressure and perturbations due to the Sun and the Moon and the observations are the raw navigation solution composed of position and receiver clock bias. Simulations and tests are done using actual data from TOPEX/POSEIDON satellite. For performance assessment, a comparison is done between the estimated state vector and the precise orbit ephemeris (POE) produced by JPL/NASA.

Key-Words: astrodynamics, artificial satellites, orbital dynamics.

1 Introduction

The Global Positioning System (GPS) is a satellite navigation system for determining position, velocity and the time (PVT) with high precision. The GPS system allows a GPS receiver to determine its position and time at any place using data signal from at least four GPS satellites (Parkinson and Spilker [10]). Using such a system, this work proposes to compute, in real time, a state vector composed of position, velocity, GPS receiver clock bias and drift of a satellite equipped with an on-board GPS receiver, by filtering the raw navigation solutions provided by the receiver. The Kalman filter is used to estimate the state vector based on such incoming observations from the receiver. The filter dynamic model includes perturbation due to geopotential, solar radiation pressure and perturbations due to the Sun and the Moon and the clock bias is modeled as a random walk process. The observations include the raw navigation solution composed of position and time bias, that are computed stepwise by the GPS receiver and provides instantaneously the absolute position. Several tests are done using three days of observations of a GPS receiver on board TOPEX/POSEIDON (T/P) satellite, which are processed by the proposed algorithm. A comparison is done between the estimated state vector and the precise orbit ephemeris (POE) produced by JPL/NASA. Current samples of satellites having an on-board GPS receiver are Kompsat (Lee et al. [8]) and BIRD (Briess [1]). Kompsat does not use the navigation solution to real time orbit determination, but for post processing orbit determination on ground. Unlikely BIRD has a receiver providing the navigation solution which is processed in real time on-board (Gill and Montenbruck [4]; Montenbruck [9]), however by an epoch state filter in conjunction with NORAD two-lines model (Hoots and Roehrich [6]). With a growing trend of on-board GPS receivers flying on upcoming satellites this work investigates characteristics of a simple real time orbit determination algorithm which could enhance the performance of the system. Also, the next generation of Brazilian satellites with no exceptions are designed to have platforms carrying GPS receivers, such as MMP (Multi-Mission Platform), LATES (Scientific Satellite), and CBERS 3 and 4 series (China Brazil Earth Resources Satellite).

With respect to the orbit determination methods, several papers can be found in the literature. The differences among them are based on the choices of the dynamic system, type of measurement and estimation technics. Some of those researchs can be found in [13], [14], [15], [16], [17], [18] and [19].

2 Methodology

The main purpose of this work is to study a rather simple but still fairly accurate algorithm to determine

the artificial satellite orbits, in real time and with low computational burden, by using the raw navigation solutions provided by GPS receivers.

The orbit determination algorithm proposed in this work is implemented by Kalman filtering of the navigation solution from a GPS receiver. The states to be estimated are the position, velocity, clock bias and clock drift of the GPS receiver on board of the spacecraft. The numerical integrator used is the fixed step Runge-Kutta of fourth order, due to its numerical stability and simplicity of use. The Kalman filter is used due to its suitability to real time applications, recursive and sequential nature, without unnecessary storage of observations, as they can be processed while being collected (Brown and Hwang [2]).

3 Dynamical Model

The dynamic model implemented in the Kalman filter is a set of first order stochastic differential equations given by:

$$\begin{aligned} \dot{\mathbf{r}} &= \mathbf{v} \\ \dot{\mathbf{v}} &= \mathbf{a} + \boldsymbol{\omega}_a \\ \dot{b} &= d \\ \dot{d} &= \omega_d \end{aligned} \tag{1}$$

where $\mathbf{r}$ is the position vector (x, y, z), $\mathbf{v}$ is the velocity vector, $\mathbf{a}$ is the acceleration, b is the bias of the GPS receiver clock, d is its drift, $\boldsymbol{\omega}_a$ is the dynamic noise on the acceleration coordinates and ω_d is the dynamic noise on the drift, characterized by white noise properties:

$$E[\boldsymbol{\omega}_a(t)] = 0; \quad E[\boldsymbol{\omega}_a(t)\boldsymbol{\omega}_a^T(\tau)] = \mathbf{Q}_a\delta(t-\tau) \tag{2}$$

$$E[\omega_d(t)] = 0; \quad E[\omega_d(t)\omega_d^T(\tau)] = Q_d\delta(t-\tau) \tag{3}$$

where $\mathbf{Q}_a$ is the spectral power density of the white noise $\boldsymbol{\omega}_a$, $\delta(t-\tau)$ is the Dirac delta equals to 1 when $t=\tau$, and zero otherwise, and Q_d is the spectral power density of the white noise ω_d.

The first order differential equations for the satellite motion, which will be integrated by using Runge Kutta method are given by:

$$\begin{aligned} \dot{\mathrm{x}}_1 &= \mathrm{x}_4 \\ \dot{\mathrm{x}}_2 &= \mathrm{x}_5 \\ \dot{\mathrm{x}}_3 &= \mathrm{x}_6 \\ \dot{\mathrm{x}}_4 &= \mathrm{a}_x \\ \dot{\mathrm{x}}_5 &= \mathrm{a}_y \\ \dot{\mathrm{x}}_6 &= \mathrm{a}_z \\ \dot{\mathrm{x}}_7 &= \mathrm{x}_8 \\ \dot{\mathrm{x}}_8 &= 0 \end{aligned} \tag{4}$$

Thus the full state vector of the filter is composed by:

$$\mathbf{x} = \begin{bmatrix} \mathrm{x} & \mathrm{y} & \mathrm{z} & \dot{\mathrm{x}} & \dot{\mathrm{y}} & \dot{\mathrm{z}} & \mathrm{b} & \mathrm{d} \end{bmatrix}^{\mathrm{T}} \tag{5}$$

or explicitly by:

$$\mathbf{x} = \begin{bmatrix} \mathrm{x}_1 & \mathrm{x}_2 & \mathrm{x}_3 & \mathrm{x}_4 & \mathrm{x}_5 & \mathrm{x}_6 & \mathrm{x}_7 & \mathrm{x}_8 \end{bmatrix}^{\mathrm{T}} \tag{6}$$

The acceleration vector a includes the geopotential effect which can be truncated to any order and degree. In real time computational environment it is noticed that the inclusion of high order terms of geopotential as well as other sources of perturbation may lead to unnecessary computational burden without the corresponding improvement in accuracy. Also, it is known that for short term predictions (30 minutes) the other sources of perturbation, including Sun and Moon third body effects, solar radiation pressure, and atmospheric drag (for LEO satellites) can be safely neglected (Gill and Montenbruck [4]).

4 Measurements Model

The measurement model of the Kalman filter algorithm is given by:

$$\mathbf{y}_k = \mathbf{H}_k\mathbf{x}_k + \mathbf{v}_k \tag{7}$$

where $\mathbf{y}$ = (x, y, z, b) is the observation vector obtained from the navigation solution provided by the GPS receiver at every sampling rate, b is the clock bias and the constant sensitivity matrix $\mathbf{H}$ is therefore given by:

$$\mathbf{H}_k = \begin{bmatrix} \mathbf{I}_{3x3} & \mathbf{0}_{3x3} & \mathbf{0}_{3x1} & \mathbf{0}_{3x1} \\ \mathbf{0}_{1x3} & \mathbf{0}_{1x3} & 1 & 0 \end{bmatrix} \tag{8}$$

The white noise vector **v** which represents the random errors of the measurements is modeled by:

$$E[\mathbf{v}_k] = 0; \quad E[\mathbf{v}_k \mathbf{v}_j^T] = \mathbf{R}_k \delta_{kj} \tag{9}$$

where δ_{kj} is the Kronecker delta which is equals to 1 when $k = j$ and zero otherwise, and the observation error covariance matrix R is given by:

$$\mathbf{R} = diag[\sigma^2 \quad \sigma^2 \quad \sigma^2 \quad \sigma^2] \tag{10}$$

with fixed $\sigma \equiv 30$m when the DOP (Dilution of Precision) information is not available from the receiver. When the DOP information is available, it is possible to form the matrix R in a more sistematic way. The following definitions are classic:

$$\sigma_r = \sigma_\rho \mathrm{PDOP} \tag{11}$$

$$\sigma_b = \sigma_\rho \mathrm{TDOP} \tag{12}$$

where σ_ρ is the standard deviation of the pseudorange measurement, PDOP is the dilution of precision in position and TDOP is the dilution of precision in time, $\sigma_\mathbf{r}$ is the standard deviation in position 3D and $\sigma_\mathbf{b}$ is the standard deviation in the bias time. Assuming that:

$$\sigma_\mathbf{r} \cong (\sigma_x^2 + \sigma_y^2 + \sigma_z^2)^{1/2}, \tag{13}$$

and since there is no better criteria, assuming also that:

$$\sigma_{x_i} = \sigma_x = \sigma_y = \sigma_z, \tag{14}$$

we have:

$$\sigma_{x_i}^2 = \sigma_r^2 / 3 \tag{15}$$

So, according to Eq. (11), we have:

$$\sigma_{x_i}^2 = \frac{\sigma_r^2}{3} = \sigma_\rho^2 \frac{\mathrm{PDOP}^2}{3}$$

or

$$\sigma_{x_i} = \frac{\sigma_\rho \mathrm{PDOP}}{\sqrt{3}} \tag{16}$$

So the matrix R (errors of the navigation solution) can be calculated by:

$$\mathbf{R} = diag\left[\left(\frac{\sigma_\rho \mathrm{PDOP}}{\sqrt{3}}\right)^2, \left(\frac{\sigma_\rho \mathrm{PDOP}}{\sqrt{3}}\right)^2, \left(\frac{\sigma_\rho \mathrm{PDOP}}{\sqrt{3}}\right)^2, (\sigma_\rho \mathrm{TDOP})^2\right] \tag{17}$$

when PDOP and TDOP are available in the navigation solution. Refers to Parkinson and Spilker [10] for several DOP definitions.

5 Transition Matrix

Another potential source of computer burden is the evaluation of the transition matrix arising from the variational equations of the orbital motion. It was noticed that more complex computation, e.g. including J2 (geopotential coefficient representing the Earth oblateness) or other effects, does not pay off in real time algorithms (Gill and Montenbruck [4]; Chiaradia et al. [3]). Owing to this, in the calculation of the transition matrix, size 8 x 8, it was only considered the Keplerian motion in the partition due to geopotential. The Keplerian transition matrix is quickly computable (Kuga [7]) with the advantage of having analytical solution (Goodyear [5]; Shepperd [11]). The full transition matrix is given by:

$$\boldsymbol{\varphi}(t, t_0) = \begin{pmatrix} \boldsymbol{\varphi}_{11} & \boldsymbol{\varphi}_{12} & \boldsymbol{\varphi}_{13} & \boldsymbol{\varphi}_{14} \\ \boldsymbol{\varphi}_{21} & \boldsymbol{\varphi}_{22} & \boldsymbol{\varphi}_{23} & \boldsymbol{\varphi}_{24} \\ \boldsymbol{\varphi}_{31} & \boldsymbol{\varphi}_{32} & \varphi_{33} & \varphi_{34} \\ \boldsymbol{\varphi}_{41} & \boldsymbol{\varphi}_{42} & \varphi_{43} & \varphi_{44} \end{pmatrix}$$

$$\equiv \begin{pmatrix} \frac{\partial \mathbf{r}}{\partial \mathbf{r}_0} & \frac{\partial \mathbf{r}}{\partial \mathbf{v}_0} & \frac{\partial \mathbf{r}}{\partial b_0} & \frac{\partial \mathbf{r}}{\partial d_0} \\ \frac{\partial \mathbf{v}}{\partial \mathbf{r}_0} & \frac{\partial \mathbf{v}}{\partial \mathbf{v}_0} & \frac{\partial \mathbf{v}}{\partial b_0} & \frac{\partial \mathbf{v}}{\partial d_0} \\ \frac{\partial b}{\partial \mathbf{r}_0} & \frac{\partial b}{\partial \mathbf{v}_0} & \frac{\partial b}{\partial b_0} & \frac{\partial b}{\partial d_0} \\ \frac{\partial d}{\partial \mathbf{r}_0} & \frac{\partial d}{\partial \mathbf{v}_0} & \frac{\partial d}{\partial b_0} & \frac{\partial d}{\partial d_0} \end{pmatrix} \tag{18}$$

The submatrices $\boldsymbol{\varphi}_{11}$, $\boldsymbol{\varphi}_{12}$, $\boldsymbol{\varphi}_{21}$, and $\boldsymbol{\varphi}_{22}$ correspond to the Keplerian motion; $\boldsymbol{\varphi}_{13}$, $\boldsymbol{\varphi}_{14}$, $\boldsymbol{\varphi}_{23}$, $\boldsymbol{\varphi}_{24}$, $\boldsymbol{\varphi}_{31}$, $\boldsymbol{\varphi}_{32}$, $\boldsymbol{\varphi}_{41}$ and $\boldsymbol{\varphi}_{42}$ are null and the remaining elements are related to bias and drift of the GPS receiver clock. This partition is given by:

$$\begin{pmatrix} \varphi_{33} & \varphi_{34} \\ \varphi_{43} & \varphi_{44} \end{pmatrix} = \begin{bmatrix} 1 & \Delta t \\ 0 & 1 \end{bmatrix} \quad (19)$$

where Δt is the time interval between observations.

6 Dynamic noise calculation

The dynamic noise matrix needed to calculate the propagated convariance matrix is given by:

$$\mathbf{\Gamma}_{\mathrm{k}}\mathbf{Q}_{\mathrm{k}}\mathbf{\Gamma}_{\mathrm{k}} = \int_{t_{k-1}}^{t_k} \varphi(t_k, t_{k-1})\mathbf{G}(t)\mathbf{Q}(t)\mathbf{G}^T(t)\varphi^T(t_k, t_{k-1})dt \quad (20)$$

To calculate the matrix G, we have the following:

$$\dot{\mathbf{x}} = \mathbf{f}(\mathrm{x}) + \mathbf{G}\boldsymbol{\omega} \quad (21)$$

it means, Eq (1) can be written like:

$$\begin{bmatrix} \dot{\mathbf{r}} \\ \dot{\mathbf{v}} \\ \dot{\mathrm{b}} \\ \dot{\mathrm{d}} \end{bmatrix} = \left[\mathbf{f}(\mathbf{r}, \mathbf{v}, \mathrm{b}, \mathrm{d})\right] + \mathbf{G}\begin{bmatrix} \boldsymbol{\omega}_{\mathrm{a}} \\ \boldsymbol{\omega}_{\mathrm{d}} \end{bmatrix} \quad (22)$$

where $\boldsymbol{\omega}_{\mathrm{a}}$ is a 3 component vector. Since $\mathbf{G}\boldsymbol{\omega}$ is explicitly given by:

$$\mathbf{G}\boldsymbol{\omega} = \begin{pmatrix} 0 & 0 & 0 & \omega_a & \omega_a & \omega_a & 0 & \omega_d \end{pmatrix}^T \quad (23)$$

we have that $\mathbf{G}$ is given by:

$$\mathbf{G} = \begin{bmatrix} 0_{3\mathrm{x}3} & 0 \\ \mathrm{I}_{3\mathrm{x}3} & 0 \\ 0_{1\mathrm{x}3} & 0 \\ 0_{1\mathrm{x}3} & 1 \end{bmatrix} \quad (24)$$

and

$$\mathbf{Q} = \mathrm{diag}\left[\sigma_{\mathrm{v}}^2 \quad \sigma_{\mathrm{v}}^2 \quad \sigma_{\mathrm{v}}^2 \quad \sigma_{\mathrm{d}}^2\right] \quad (25)$$

with $\mathrm{E}[\boldsymbol{\omega}_{\mathrm{a}}^2] = \sigma_{\mathrm{a}}^2$ e $\mathrm{E}[\boldsymbol{\omega}_{\mathrm{d}}^2] = \sigma_{\mathrm{d}}^2$.

To solve Eq. (20) it is defined:

$$\mathrm{I1} = \varphi_{\mathrm{k,k}}\mathbf{GQG}^{\mathrm{T}}\varphi_{\mathrm{k,k}}$$

$$\mathrm{I2} = \varphi_{\mathrm{k,k-1}}\mathbf{GQG}^{\mathrm{T}}\varphi_{\mathrm{k,k-1}} \quad (26)$$

Then, the addtion of the dynamic noise matrix is calculated by the trapeze rule, and it is givem by:

$$\mathbf{\Gamma}_{\mathrm{k}}\mathbf{Q}_{\mathrm{k}}\mathbf{\Gamma}_{\mathrm{k}} \cong \frac{1}{2}(\mathrm{I1} + \mathrm{I2})\Delta\mathrm{t} \quad (27)$$

with $\varphi_{\mathrm{k,k}} = \mathrm{I}$ e $\varphi_{\mathrm{k,k-1}}$ given by:

$$\varphi = \begin{bmatrix} \phi_{6x6} & 0_{6x2} \\ 0_{2x6} & \begin{matrix} 1 & \Delta t \\ 0 & 1 \end{matrix} \end{bmatrix} \quad (28)$$

where φ_{6x6} was calculated like section 5.

7 Simulations Data

For the test cases, data from the TOPEX/POSEIDON satellite, from November 1993 was used. The results were compared to the POE (Precision Orbit Ephemeris) files, which are released by JPL/NASA in Internet.

To start the procedure it is used the two first navigation solutions provided by the GPS receiver to generate the initial states of the filter (position, velocity, bias and null drift). The standard Kalman filter algorithm was implemented (Brown and Hwang [2]), where the time update cycle used the transition matrix as proposed by Eq. 18 to compute the predicted covariance. The measurement update cycle used the conventional Kalman form to process the navigation solution observations in a sequential manner.

Table 1 shows the filter initial state error covariance matrix, where σ represents the standard deviation. These values were used throughout the tests. Table 2 shows the values of dynamic noise covariance matrices $\boldsymbol{Q}_a$ and Q_d used in the filter. The measurement errors were set as in Eq. 10 or 11.

Table 1: Initial Covariance

Parameter	Initial Value
Position σ^2 - $\boldsymbol{P}_r$ (m)^2	diag (1000^2)
Velocity σ^2 - $\boldsymbol{P}_v$ (m/s)^2	diag (10^2)
Bias σ^2 - P_b (m)^2	1000^2
Drift σ^2 - P_d (m/s)^2	10^2

Table 2: Dynamic Noise Covariance

Parameter	Value
$\boldsymbol{Q}_a$ $(m/s^2)^2$	diag $(0.5)^2$
Q_d $(m/s^2)^2$	0.5^2

6 Results

Many tests are performed in Gomes [12] concerning the time interval that the observations are available and also the different degree and order of the geopotential harmonic coeficients. In that work it was only considered the perturbation due to the geopotential. Table 3 shows the residuals in position and bias coordinates for all cases tested.

Table 3: Residual Statictics – 19/11/93

Integ. step(s)	Model	Residual (m)			
		x	y	z	bias
10	Kepl.	0,012 ± 10,640	0,035 ± 8,111	0,015 ± 19,326	-0,020 ± 12,426
	J_2	0,001 ± 10,494	-0,001 ± 7,950	-0,001 ± 19,259	-0,020 ± 12,426
	10 x 10	0,001 ± 10,494	0,001 ± 7,950	-0,002 ± 19,259	-0,020 ± 12,426
	50 x 50	0,001 ± 10,494	0,001 ± 7,950	-0,002 ± 19,259	-0,020 ± 12,426
60	Kepl.	0,144 ± 38,007	0,420 ± 30,649	0,188 ± 58,028	-0,947 ± 44,231
	J_2	0,003 ± 31,918	-0,001 ± 24,138	0,017 ± 54,873	-0,947 ± 44,231
	10 x 10	0,001 ± 31,917	0,021 ± 24,138	0,005 ± 54,872	-0,947 ± 44,231
	50 x 50	0,000 ± 31,917	0,022 ± 24,138	0,006 ± 54,873	-0,947 ± 44,231
300	Kepl.	-1,413 ± 470,528	11,813 ± 438,534	1,674 ± 423,275	-0,030 ± 50,730
	J_2	-0,405 ± 62,013	-0,078 ± 28,715	0,110 ± 62,654	-0,030 ± 50,729
	10 x 10	-0,458 ± 61,843	0,450 ± 28,343	-0,127 ± 62,578	-0,030 ± 50,729
	50 x 50	-0,442 ± 61,825	0,454 ± 28,337	-0,124 ± 62,586	-0,030 ± 50,729
600	Kepl.	-71,934±2341,234	28,673 ±1274,758	-36,383 ± 2123,751	0,030 ± 57,982
	J_2	-52,464 ± 1586,162	-15,894 ± 715,830	-20,933 ± 1564,720	0,030 ± 57,982
	10 x 10	-52,322 ± 1586,465	-13,903 ± 714,839	-21,952 ±1565,111	0,030 ± 57,982
	50 x 50	-52,240 ± 1586,635	-13,886 ± 714,890	-21,923 ± 1565,002	0,030 ± 57,982

Tables 4 shows the statistics of error in position and velocity in the orbit determination process, for four different interval of observations and harmonic coefficient models. From those range of tests it is concluded that it is advisable to model at least the J2 effect in the satellite orbital motion, when sampling rates from 10 seconds to 5 minutes are used.

Table 4: Statistics of error in orbit determination– 19/11/93

Integ. Step (s)	**Model**	**Error in position (m)**		
		x	*y*	*z*
10	**Kepl**	-2,608 ± 27,438	-4,310 ± 33,422	1,434 ± 37,357
	J_2	-2,612 ±27,429	-4,323 ± 33,402	1,428 ± 37,385
	10 x 10	-2,612 ± 27,428	-4,322 ± 33,402	1,428 ± 37,385
	50 x 50	-2,612 ± 27,428	-4,322 ± 33,402	1,428 ± 37,385
60	**Kepl**	-2,195 ± 27,260	-4,420 ± 33,573	1,439 ± 35,961
	J_2	-2,197 ± 27,255	-4,426 ± 33,559	1,437 ± 35,975
	10 x 10	-2,197 ± 27,255	-4,426 ± 33,559	1,437 ± 35,975
	50 x 50	-2,197 ± 27,255	-4,426 ± 33,559	1,437 ± 35,975
300	**Kepl**	-2,685 ± 24,493	-3,899 ± 29,842	0,901 ± 38,966
	J_2	-2,684 ± 24,497	-3,800 ± 32,027	1,461 ± 29,765
	10 x 10	-2,684 ± 24,497	-3,800 ± 32,027	1,449 ± 29,759
	50 x 50	-2,684 ± 24,497	-3,800 ± 32,027	1,448 ± 29,759
600	**Kepl**	-3,203 ± 22,153	-3,907 ± 104,954	1,984 ± 314,483
	J_2	-3,198 ± 22,191	-3,445 ± 72,168	4,884 ± 140,561
	10 x 10	-3,198 ± 22,191	-3,460 ± 72,201	4,676 ± 140,645
	50 x 50	-3,198 ± 22,191	-3,461 ± 72,210	4,674 ± 140,664
Integ. Step (s)	**Model**	**Error in velocity (m/s)**		
		Vx	*Vy*	*Vz*
10	**Kepl**	0,0006 ± 0,4839	0,0018 ± 0,3561	-0,0002 ± 0,8368
	J_2	0,0001 ± 0,4761	0,0001 ± 0,3416	-0,0009 ± 0,8333
	10 x 10	0,0001 ± 0,4761	0,0002 ± 0,3416	-0,0010 ± 0,8333
	50 x 50	0,0001 ± 0,4761	0,0002 ± 0,3416	-0,0010 ± 0,8333
60	**Kepl**	0,0012 ± 0,3905	0,0036 ± 0,3098	0,0008 ± 0,5612
	J_2	0,0000 ± 0,3491	0,0001 ± 0,2501	-0,0006 ± 0,5385
	10 x 10	0,0000 ± 0,3491	0,0003 ± 0,2502	-0,0007 ± 0,5385
	50 x 50	0,0000 ± 0,3491	0,0003 ± 0,2502	-0,0007 ± 0,5385
300	**Kepl**	0,0065 ± 0,8238	0,0210 ± 0,7894	-0,0013 ± 0,7726
	J_2	0,0085 ± 0,2830	0,0005 ± 0,1275	-0,0013 ± 0,2756
	10 x 10	0,0084 ± 0,2828	0,0014 ± 0,1275	-0,0017 ± 0,2754
	50 x 50	0,0084 ± 0,2828	0,0014 ± 0,1275	-0,0017 ± 0,2754
600	**Kepl**	0,1537 ± 4,3683	0,0430 ± 2,0999	-0,0487 ± 4,1250
	J_2	0,1504 ± 4,2184	0,0024 ± 1,7322	-0,0337 ± 3,8230
	10 x 10	0,1502 ± 4,2185	0,0042 ± 1,7319	-0,0345 ± 3,8235
	50 x 50	0,1503 ± 4,2185	0,0043 ± 1,7319	-0,0345 ± 3,8234

In the following results presented here, the basic model considers the geopotential up to 10 x 10. On this model it is added the solar radiation pressure and the Sun and Moon gravitational effects.

Table 5 shows the statistic errors (mean and standard deviation) in position and velocity in the orbit determination process, using different perturbations model and also different degree and order truncation of the harmonic coefficients.

Model 1: geopotential up to 10 x 10 (basic)

Model 2: geopotential up to 10 x 10 + Sun + Moon + solar radiation pressure

Model 3: geopotential up to 50 x 50 + Sun + Moon + solar radiation pressure

Table 5: Statistc errors in the orbit determination 19/11/93

Model	**Position Error (m)**		
	x	*y*	*z*
1	-2.6121293 ± 27.4285067	-4.3222859 ± 33,4019768	1.4279681 ± 37.3849305
2	-2,6121327 ± 27.4285099	-4.3222926 ± 33.4019467	1.4279669 ± 37.3849280
3	-2,6121079 ± 27.4284953	-4.3222804 ± 33.4019381	1.4279734 ± 37.3849385
Model	**Velocity Error (m/s)**		
	Vx	*Vy*	*Vz*
1	0.0000702 ± 0.4761041	0.0002127 ± 0.3416321	-0.0010083 ± 0.8333067
2	0.0000694 ± 0.4761042	0.0002106 ± 0.3416309	-0.0010081 ± 0.8333069
3	0.0000726 ± 0.4761042	0.0002150 ± 0.3416274	-0.0010086 ± 0.8333065

The results show that the inclusion of the perturbations due to the Sun, the Moon and solar radiation pressure, as well as the higher degree and order of the harmonic coefficients, have positive effects in the error reduction, however with rather limited improvement. Taking into account that the processing time increases when these perturbations are added and the focus is real time application, in general, the added complexity of those models are not justified.

In this way, Figs. 1 and 2 show the mean error in position and velocity, using the model considering just the geopotential up to 10 x 10. It is observed that the mean error in position is smaller than 4.5 m and the standard deviation is smaller than 37.5 m. The mean error in velocity is smaller than 0.2 mm/s and the standard deviation is smaller than 0.8 m/s.

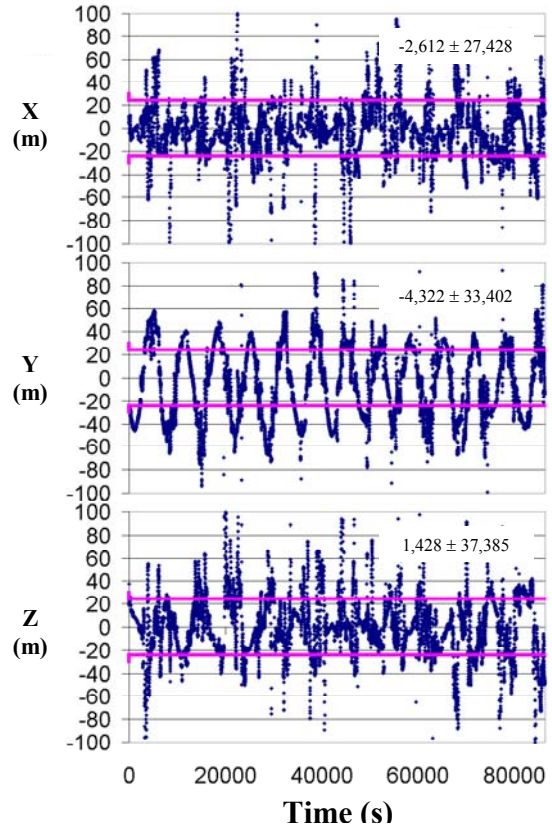

Figure 1 – Error in position

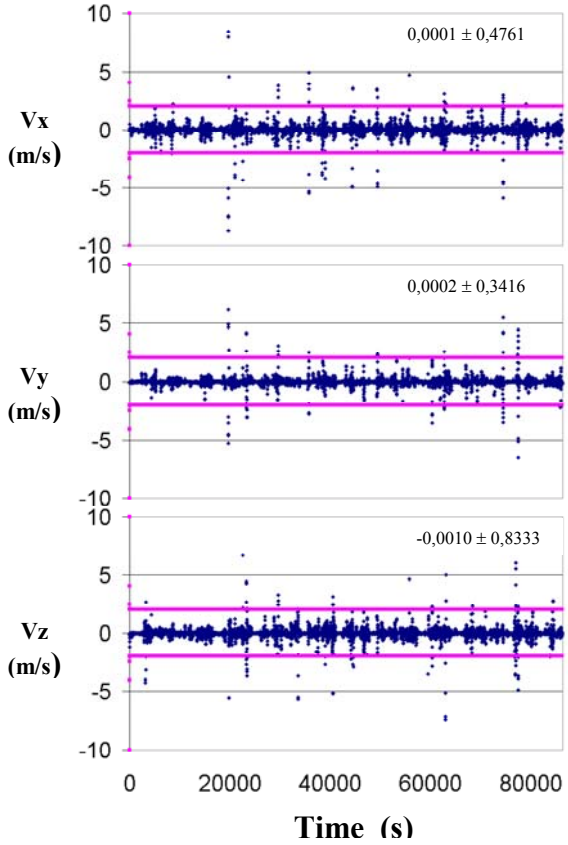

Figure 2 – Error in velocity

7 Conclusion

In this work it was analysed the influence in the dynamic model and the integration step in the orbit determination process, in real time and using the GPS navigation solution. Perturbations due to the Sun, the Moon and the solar radiation pressure were included in the orbit determination and results show that these perturbations must be included only in the case when very higy accuracy is required.

Apart from this, these perturbations also increase the CPU time, which is a disadvantage in real time process. These errors are consistent with the observations errors (navigation solution) which were assumed by the Kalman filter, it means, standard deviation of 30 m in each component.

References

[1] Briess, K. Satellitenbescheibung: BIRD Spacecraft Description. Vol. 1, DLR, Germany, 2000, TN-BIRD-1000-WP/084.

[2] Brown, R.G.; Hwang, P.Y.C. Introduction to random signals and applied Kalman filtering. New York, John Wiley, 1997.

[3] Chiaradia, A.P.; Kuga, H.K.; Prado, A.F.B.A. Investigation of simplified models for orbit determination using single frequency GPS measurements. Journal of the Brazilian Society of Mechanical Sciences RBCM, Vol. XXI, p. 165-172, 1999.

[4] Gill, E.; Montenbruck, O. On-board navigation system for the BIRD small satellite. DLR, Germany, 2002, Forschungsbericht 2002-06.

[5] Goodyear, W.H. Completely general closed form solution for coordinates and partial derivatives of the two-body problem. The Astronomical Journal, 70(3), p. 189-192, Apr. 1965.

[6] Hoots, F.R.; Roehrich, R.L. Models for propagation of NORAD element sets. Aerospace Defense Command, USAF, Dec. 1980, Project Spacecraft Report 3.

[7] Kuga, H.K. Transition matrix of the elliptical Keplerian motion. São Jose dos Campos, INPE, Jan. 1986, Internal report INPE-3779-NTE/250 (in portuguese).

[8] Lee, B.S.; Lee, J.S.; Kim, J.H.; et al. Reconstruction of KOMPSAT-1 GPS navigation solutions using GPS data generation and preprocessing program. Acta Astronautica, 54, p. 571-576, 2004.

[9] Montenbruck, O. An epoch state filter for use with analytical orbit models of low Earth satellites. Aerospace Science and Technology, 4, p. 277-287, 2000.

[10] Parkinson, B.W.; Spilker Jr., J.J. Global Positioning System: theory and applications. AIAA, Vol. 1, 1996 (Progress in Astronautics and Aeronautics 163).

[11] Shepperd, S.W. Universal Keplerian state transition matrix. Celestial Mechanics, 35, p. 129-144, 1985.

[12] Gomes, V. M. Orbit determination of artificial satellites in real time through the navigation solution of GPS. 2004. 107p. (INPE-14649-TID/1208). Master Dissertation, INPE, São José dos Campos, 2004 (in portuguese).

[13] Kuga, H. K. Determinação de órbitas de satélites artificiais terrestres através de técnicas de estimação combinadas a técnicas de suavização de estado. 1989. 249p. (INPE-4959-TDL/079). PhD Thesis (Doutorado em Ciência Espacial/Mecânica Orbital) - Instituto Nacional de Pesquisas Espaciais, São José dos Campos, 1989. (in portuguese)

[14] Paiva, R. N. Determinação autônoma de órbita usando GPS.1988. 230p. (INPE-4815-TDL/361). PhD Thesis (Doutorado em CEA/Mecânica Orbital) - Instituto Nacional de Pesquisas Espaciais, São José dos Campos, 1988. (in portuguese)

[15] Bertiger, W.I; Bar-Server, Y.E.; Christensen, E.J.; Davis, E.S.; Guinn, J.R.; Haines, B.J.; Ibanez-Meier, R.W.; Jee, J.R.; Lichten, S.M.; Melbourne, W.G.; Muellerschoen, R.J.; Munson, T.N.; Vigue, Y.; Wu, S.C.; Yunck, T.P.; Schutz, B.E.; Abusali, P.A.M.; Rim, H.J.; Watkins, M.M.; Willis, P. GPS precise tracking of TOPEX/Poseidon: results and implications. Journal of Geophysical Research. v. 99, n. C12, p. 24449-24463, Dec. 1994.

[16] Binning, P. W. GPS, dual frequency, SA free satellite navigation. In: ION Annual Meeting, 52. Boston, 1996. Anais… Alexandria: The Institute of Navigation. p. 803-812.

[17] Galski, R. L.; Orlando, V.; Kuga, H. K. Autonomous orbit control procedure, using a simplified GPS navigator, applied to the CBERS satellite. In: INTERNATIONAL SYMPOSIUM ON SPACE FLIGHT DYNAMICS, 16., 2001, Pasadena, USA. Proceedings... 2001. (INPE-9573-PRE/5203).

[18] Chiaradia, A.P.M.; Kuga, H.K.; Prado, A.F.B.A. Single frequency gps measurements for real time determination of artificial satellite orbit. In: Othon C. Winter e A. F. Bertachini A. Prado (ed.) Advances in space dynamics 3 applications in astronautics. São José dos

Campos: INPE, 2002. ISBN: 85-85-17-00006-4, p. 88-99.

[19] Lopes, R. V. F.; Kuga, H. K. ORBEST - A GPS navigation solution algorithm without DOP analysis. In: Howell, K. C.; Cicci, D. A.; Cochran Jr, J. E.; Kelso, T.S. (ed.) Advances in the Astronautical Sciences. Huntsville, Alabama: American Astronautical Society, 1997. AAS97-108, v. 95, n.1, p. 153-166.